

Extended Energy Elemental Spectrum Measurements with the Solar Isotope Spectrometer (SIS)

A. W. Labrador^a, C. M. S. Cohen^a, A. C. Cummings^a, R. A. Leske^a, R. A. Mewaldt^a, E. C. Stone^a, T. T. von Rosenvinge^b, M. E. Wiedenbeck^c.

(a) California Institute of Technology, MC 220-47, Pasadena, CA 91125 USA

(b) NASA/Goddard Space Flight Center, Greenbelt, MD 20771 USA

(c) Jet Propulsion Laboratory, Pasadena, CA 91109 USA

Presenter: A. W. Labrador (labrador@srl.caltech.edu), usa-labrador-AW-abs2-sh12-poster

The Solar Isotope Spectrometer (SIS) aboard the Advanced Composition Explorer (ACE) has been measuring solar energetic particle abundances since ACE was launched in August 1997. SIS is a silicon detector telescope that identifies charged particles via the multiple dE/dx vs. total energy technique, and to date, most measurements reported by SIS have been limited in energy to those particles that stop in the instrument. In this paper, we will summarize the multiple dE/dx technique used to identify particles that penetrate through the bottom of SIS, extending the energy ranges for elemental abundance measurements. In preliminary analysis, the upper energy limit for oxygen has been extended from ~90 MeV/nuc for stopping particles to ~300 MeV/nuc for penetrating particles, and the upper energy limit for iron has been extended from ~168 MeV/nuc to ~500 MeV/nuc. We apply this technique to SIS measurements of large SEP events, such as the Nov. 6, 1997 event and the recent Jan. 20, 2005 event, to extend the measured spectra, to look for evidence of spectral breaks.

1. Introduction

The Solar Isotope Spectrometer (SIS) aboard the Advanced Composition Explorer (ACE) has been measuring solar energetic particle spectra since ACE launched in 1997. SIS is a silicon detector telescope which identifies charged particles and their energies via the ΔE vs E' ("residual E' ") technique, and energy spectra reported by SIS have been limited to date to those particles that stop in the instrument. Although stopping particles are required for isotope resolution, elemental spectra can be obtained at higher energies with penetrating particles.

The SIS instrument is composed of two identical silicon detector stacks, each topped by a pair of position sensitive matrix detectors to provide trajectory information for particles entering the instrument. The matrix detectors are 70-80 μm thick, with 33.9 cm^2 active area. Each stack beneath the matrix detectors is composed of 15 high purity silicon detectors, of $\sim 65 \text{ cm}^2$ active area and of individual thicknesses varying from 0.1 mm to 1 mm, and the individual detectors are collected in groups of 1 to 6 of the individual silicon detectors, for a total of 8 detector groups per stack. The detector groups are labeled T1 through T8. The instrument is described in detail in [1].

Particles entering the instrument through the matrix detectors are assigned a range flag (RNG) corresponding to the deepest detector in the stack that triggers, so that a particle that stops in T7 is assigned a range of 7. Higher energy particles that enter T8 and stop in it or pass entirely through it are RNG 8 and are considered penetrating. The first panel of Figure 1 shows expected ΔE vs. E' response curves for stopping and penetrating oxygen and iron in the SIS instrument. In this case, ΔE is the measured energy deposited in T1 through T5, and E' is the measured energy deposited in T6 through T7, although other combinations of detectors are possible. The fold-back point on each curve represents the point at which a particle leaves T7

and enters T8. The penetrating particle portions of the curves continue down and to the left until minimum ionizing energies are reached, at which point the curves fold back again along a minimum ionizing diagonal.

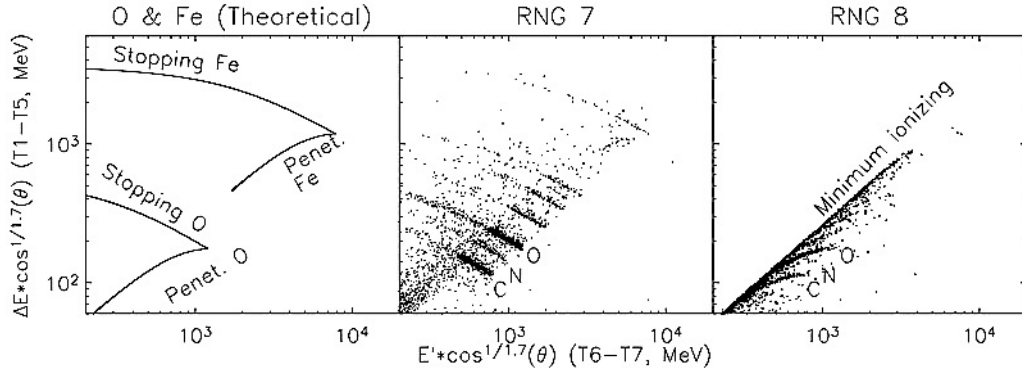


Figure 1: ΔE vs E' data measured by SIS. The left panel shows expected O and Fe curves for stopping and penetrating particles. The center and right panels show flight data for the 6 November 1997 event. C, N, and O are identified.

The center and right panels of Figure 1 show samples of flight data, from the 20 January 2005 SEP event, for RNG 7 and RNG 8 particles. Even with no charge consistency or tracking quality cuts applied to these plots, elements and, in some cases, isotopes can be clearly identified in stopping particle data, and elements remain separated in penetrating particle data for an extended energy range.

2. Discussion

Penetrating particle algorithms for this analysis were derived from similar algorithms developed for the CRIS instrument [2]. As in that analysis, the penetrating particle analysis involves first selecting particles by element (Z), then determining energies for each particle given its assumed charge (Z) and mass (A), and finally forming spectra. This analysis takes advantage of the clear charge separation provided by the SIS instrument for penetrating particles, as is evident in the right panel of Figure 1, so that element identification is simply a matter of mapping cuts to the RNG 8 ΔE vs E' data and selecting for whatever Z is under consideration. Penetrating particle tracks in the RNG 8 ΔE vs E' plot begin to merge as energies approach minimum ionizing, so it is also important to select for particles well to the right of the minimum ionizing band, in order to prevent or minimize contamination of particle counts by adjacent elements.

Once particles have been selected for a given Z and assumed A , we apply a range-energy relationship for protons passing through silicon and scaled for higher Z in order to estimate energies for individual particles [3-5]. Energies are calculated by comparing predicted detector responses vs. E for given charge Z and mass A with the measured detector responses, taking into account measured angles of incidence and choosing the best fit via chisquare. While the CRIS penetrating particle analysis takes into account detector dead layers, the dead layers in SIS are negligible.

A test of the energy-measurement algorithm for penetrating particles can be obtained by treating RNG 7 stopping particles as "penetrating" and ignoring the energy deposited in the T7 and T8 detectors. Figure 2 shows energy ranges for RNG 7 and RNG 8 as horizontal, cross-hatched bars, calculated using the penetrating particle algorithm applied to a large sample of quiet time data. The black bar at the top shows the corresponding RNG 7 energy range for stopping-particle analysis. The energy histograms shown are from the 20 January 2005 event, for visual comparison. The figure shows good agreement between RNG 7

energy ranges obtained via the two techniques, demonstrating reasonably acceptable accuracy for the penetrating particle analysis. Figure 3 shows how penetrating particles may extend the total energy range of the SIS instrument for selected elements, using a large sample of quiet-time data. The oxygen energy range may be extended to ~ 300 MeV/nuc, and iron may extend to as high as ~ 500 MeV/nuc. However, for particular SEP events, the energy ranges may not extend as high, due to lower counting statistics for specific elements.

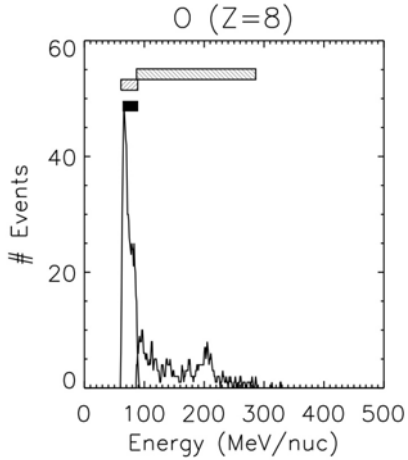


Figure 2: Sample oxygen energy histograms for RNG 7 and RNG 8 using the penetrating particle algorithm. The energy ranges were calculated using a sample of quiet-time data, while the histograms are from the 20 January 2005 event, for comparison.

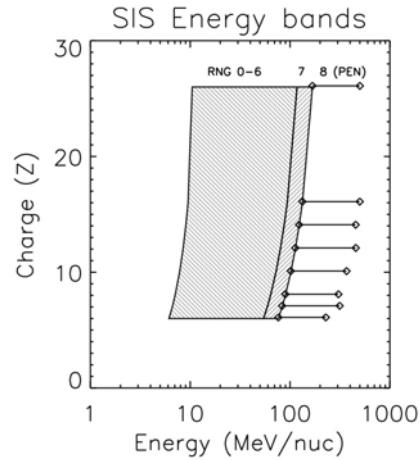


Figure 3: SIS energy ranges for $Z=6-26$. Shown are energy ranges for stopping particles (RNG 0-6) and penetrating particles. Penetrating particle energies were obtained from a sample of quiet-time data.

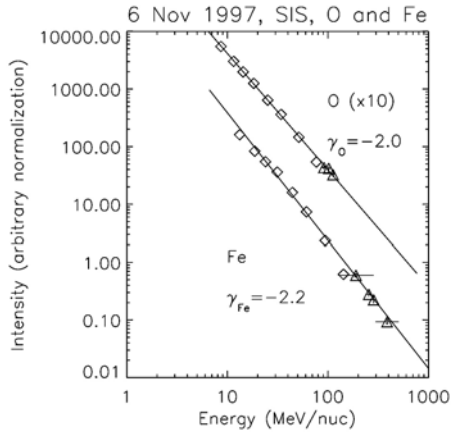


Figure 4: Stopping particle (open diamonds) and penetrating particle (open triangles) intensities for O and Fe, for the 6 Nov 1997 SEP event.

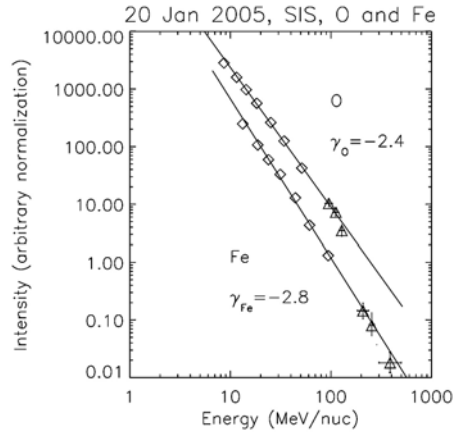


Figure 5: Stopping particle (open diamonds) and penetrating particle (open triangles) intensities for O and Fe, for the 20 Jan 2005 SEP event.

Figures 4 and 5 show oxygen and iron spectra for the 6 Nov. 1997 and 20 Jan. 2005 SEP events. Both were large SEP events characterized in part by hard power law spectra ($\gamma \sim -2$ to -2.8) to high energies for a variety of elements. Hard cuts were applied to the penetrating oxygen data in order to reduce contamination of the measurement from adjacent elements, so the oxygen energy ranges extend only as high as ~ 150 MeV/nuc. Also, at this stage of development, analysis has not been completed to obtain absolute intensities for penetrating particles, so the penetrating particle intensities are scaled to lie along projections from the stopping particle intensities.

However, although the absolute intensities have not yet been obtained for penetrating particles, the relative intensities for points within the penetrating particle energy ranges may be used to look for evidence of softening or hardening of spectra relative to the stopping particle spectra. In the case of the 6 Nov 1997 event, a projection of a power-law fit to the Fe stopping spectrum passes through all the penetrating Fe intensities and error bars. Stopping data for the 20 Jan 2005 spectra hint at a steepening in Fe, but the penetrating Fe points can be scaled simultaneously to lie very close to the power-law projected fit. For the 20 Jan 2005 event, RNG 7 and RNG 8 Fe exhibit significant overlap in energies near the transition from stopping to penetrating, and these events have not yet been combined into a single point on the spectrum.

3. Conclusions

As with data from the CRIS instrument, penetrating particles in SIS data show clear separation of elements up to significantly higher energies than are available with stopping particles alone. The penetrating particle analysis developed for the CRIS instrument has been adapted to analysis of SIS penetrating particle data, and tests of the penetrating particle algorithm on stopping particle data demonstrate that the analysis should result in reasonably accurate particle energies. Further analysis is called for in order to obtain absolute intensities for penetrating particles in SIS data.

4. Acknowledgements

This work was supported by NASA grant NAG5-6912.

References

- [1] E. C. Stone, et al., Space Sci. Rev., 86, 357 (1998).
- [2] A. W. Labrador, et al., Proc. 28th Internat. Cosmic Ray Conf., Tsukuba, 4, 1773 (2003).
- [3] S. P. Ahlen, Rev. Mod. Phys., 52, 121, (1980).
- [4] H. H. Andersen and Z. F. Ziegler, "Hydrogen: Stopping Powers and Ranges in All Elements", Volume 3 of The Stopping and Ranges of Ions in Matter (Pergamon: New York 1977).
- [5] E. C. Stone, et al., Space Sci. Rev., 96, 285 (1998).